TENSOR RECONSTRUCTION-BASED SPARSE ARRAY 2-D DOA ESTIMATION OF MIXED COHERENT AND UNCORRELATED SIGNALS

Saidur R. Pavel[†]*, Yimin D. Zhang*[†]*, Shunqiao Sun*[‡]*, and André L. F. de Almeida*[§]

[†] Department of Electrical and Computer Engineering, Temple University, Philadelphia, PA 19122, USA
[‡] Department of Electrical and Computer Engineering, The University of Alabama, Tuscaloosa, AL 35487, USA
[§] Department of Teleinformatics Engineering, Federal University of Ceara, Fortaleza, Brazil

ABSTRACT

This paper addresses the direction-of-arrival (DOA) estimation problem of mixed coherent and uncorrelated signals using a sparse rectangular array, where tensor reconstruction is employed to preserve the structure of multi-dimensional array signals. In the proposed approach, we first estimate the DOAs of uncorrelated signals using the subspace algorithm. After eliminating the contribution of uncorrelated signals from the covariance tensor, a structural tensor decorrelation process is introduced to decorrelate the resulting coherent covariance tensor. The canonical polyadic decomposition method is employed to the decorrelated covariance tensor to detect the coherent signals. The conditions of signal resolvability are analyzed.

Index Terms— Direction of arrival estimation, sparse array, tensor decomposition, Canonical polyadic decomposition, mixed coherent and uncorrelated signals

1. INTRODUCTION

Direction of arrival (DOA) estimation holds significant importance in the area of array signal processing with broad applications to wireless communication, radar, automotive vehicle, sonar, acoustic tracking, radio astronomy, and biomedical imaging [1–8]. Among the methods developed for DOA estimation, subspace-based methods, such as MUSIC [9] and ESPRIT [10], are popularly used to resolve uncorrelated signals. However, these methods cannot resolve highly correlated or coherent signals. Real-world scenarios often involve coherent signals, which frequently emerge from phenomena like multipath propagation in wireless communications to low-angle reflection in radar systems. In addition, for estimating coherent signals, decorrelation techniques based on covariance matrices, such as spatial smoothing [11, 12] and matrix reconstruction [13, 14], are popularly used.

The problem becomes further challenging when a mixture of coherent and uncorrelated signals is present. Several approaches have been developed to effectively handle both coherent and uncorrelated signals. Reference [15] considers DOA estimation for uniform linear arrays (ULAs) in a mixed coherent and uncorrelated signal scenario. The method involves initially estimating the uncorrelated signals using the MUSIC algorithm, followed by their removal through the exploitation of the symmetric properties of the ULA. Subsequently, a Toeplitz matrix is reconstructed for the remaining coherent signals. DOA estimation of mixed coherent and uncorrelated signals is considered in [16] for a multiple-input multiple-output (MIMO) radar framework where both the transmit array and the receive array are sparse ULAs forming a coprime sum coarray. The DOAs of the coherent signals are estimated using Bayesian compressive sensing [17].

Many practical sensing problems involve two-dimensional (2-D) DOA estimation to simultaneously determine both azimuth and elevation angles of signal arrivals. The methods mentioned above primarily rely on matrix-based processing. When dealing with multi-dimensional array signals using multiple snapshots, multi-dimensional signal processing relying on high-dimensional tensor modeling can be exploited to enable preservation of structural characteristics of the signals.

The inherent characteristics of tensor signals can be effectively exploited through tensor decomposition techniques. Commonly used methods for tensor decomposition include the canonical polyadic decomposition (CPD) [18, 19], the Tucker decomposition [20], and the high-order singular value decomposition (HOSVD) [21]. For instance, tensor decomposition is employed in [22] for DOA estimation in multi-dimensional ULAs. A DOA estimation approach is introduced in [23, 24] based on coarray tensors designed for multi-dimensional structured sparse arrays. It is important to note that these methods only consider uncorrelated signals. To handle coherent signals, tensor-based spatial smoothing techniques is presented in [25] and [26]. However, the repeated tensor calculations in these methods result in limited decorrelation effectiveness with a high computational overhead. In [27], the structural property of the covariance tensor is investigated to reconstruct a tensorial Hermitian and Toeplitz structure.

In this paper, we consider a mixed coherent and uncorrelated signal scenario for 2-D DOA estimation. To maintain the structural properties of the multi-dimensional signal, our approach employs tensor-based processing. The proposed procedure begins with the estimation of 2-D DOAs of the uncorrelated signals using the MUSIC algorithm. The effect of uncorrelated signals is eliminated in the covariance tensor through the utilization of the symmetric conjugate property inherent to the covariance tensor of uncorrelated signals. Subsequently, the remaining coherent covariance tensor is subjected to decorrelation using a structured tensor reconstruction method. By applying the CPD to the decorrelated coherent covariance tensor, the 2-D DOAs of the coherent signals are estimated. The effectiveness of the proposed technique is validated by theoretical analysis and simulation results.

Notations: We use lower-case, upper-case, and upper-case calligraphic bold characters to denote vectors, matrices, and tensors, respectively. In particular, $\boldsymbol{I}$ and $\boldsymbol{\mathcal{I}}$ denote the identity matrix and the identity tensor of a proper dimension, respectively. $(\cdot)^{\mathrm{T}}$ and $(\cdot)^{\mathrm{H}}$ respectively represent the transpose and Hermitian operations

The work of S. R. Pavel and Y. D. Zhang was supported in part by the National Science Foundation (NSF) under grant No. ECCS-2236023. The work of S. Sun was supported in part by the NSF under grant No. CCF-2153386.

of a matrix or a vector, and $(\cdot)^*$ denotes complex conjugate. $\circ$ and $\odot$ denote outer product and element-wise product, respectively. In addition, $\kappa(\cdot)$ represents the Kruskal rank of a matrix and $\mathbb{C}^{M\times N}$ denotes the $M \times N$ complex space. $|\mathbb{P}|$ returns the cardinality of set $\mathbb{P}$. $\mathrm{E}(\cdot)$ denotes statistical expectation.

CPD: The CPD represents a high-order tensor as a linear combination of a minimum number of rank-1 tensor components. For an N-dimensional tensor $\boldsymbol{\mathcal{A}} \in \mathbb{C}^{I_1\times I_2\times\cdots\times I_N}$, its rank-$R$ CPD can be expressed as

$$\boldsymbol{\mathcal{A}} = \sum_{r=1}^{R} \eta_r \boldsymbol{a}_1(r) \circ \boldsymbol{a}_2(r) \circ \boldsymbol{a}_N(r) \triangleq [\![\boldsymbol{\eta}; \boldsymbol{A}_1; \boldsymbol{A}_2; \boldsymbol{A}_N]\!], \quad (1)$$

where $\boldsymbol{a}_n(r) \in \mathbb{C}^{I_n}$ is a canonical polyadic (CP) factor, $\boldsymbol{A}_n = [\boldsymbol{a}_n(1), \boldsymbol{a}_n(2), \cdots, \boldsymbol{a}_n(R)] \in \mathbb{C}^{In\times R}$ denotes the corresponding factor matrix for $n = 1, 2, \cdots, N$, and $\boldsymbol{\eta} = [\eta_1, \eta_2, \cdots, \eta_R]^{\mathrm{T}}$ is a vector of scalar coefficients.

2. ARRAY AND SIGNAL MODELS

2.1. Array Geometry Model

We consider an origin-symmetric 2-D sparse rectangular array $\mathbb{S}$ as shown in Fig. 1. The X and Y axes comprise M_x and M_y sensors, respectively. In both axes, the inter-element spacing is $d = \lambda/2$ with λ denoting the wavelength of the incoming signals. $\mathbb{P}_x$ and $\mathbb{P}_y$ denote the positions of the sparsely placed sensors along the X and Y axes, respectively, and the sensor locations for the 2D array $\mathbb{S}$ is expressed as

$$\mathbb{P} = \{(x, y) \mid x \in \mathbb{P}_x, y \in \mathbb{P}_y\}. \quad (2)$$

Without any loss of generality, it is assumed that the number of sensors in each direction, i.e., M_x and M_y, is an odd number. The total number of sensors in this configuration is M_xM_y. We also define U_x and U_y such that $U_xd = \max(\mathbb{P}_x)$ and $U_yd = \max(\mathbb{P}_y)$.

2.2. Signal Model

Consider mixed coherent and uncorrelated narrowband far-field signals impinging on the array $\mathbb{S}$, where D signals are mutually uncorrelated and L signals are coherent. The L coherent signals exhibit coherence with one another but remain uncorrelated with the D uncorrelated signals. These L coherent signals impinging from azimuth and elevation angles (θ_c^l, ϕ_c^l) are scaled versions of $s_c(t)$ up to a complex scalar α_l, $l = 1, 2, \cdots, L$, whereas the waveform of the dth uncorrelated signal is denoted as $s_u^d(t)$. The total number of uncorrelated and coherent signals impinging on the array is $Q = D + L$. Note that we use subscripts c and u to denote coherent and uncorrelated signals, respectively.

For a signal impinging from azimuth angle θ and elevation angle ϕ, the steering vectors in the X and Y directions for the array $\mathbb{S}$ are respectively expressed as

$$\begin{aligned}\boldsymbol{a}(\mu) &= [e^{-j\pi\mathbb{P}_{(x,0)}\mu}, \cdots, e^{-j\pi\mathbb{P}_{(x,M_x-1)}\mu}]^{\mathrm{T}} \in \mathbb{C}^{M_x},\\ \boldsymbol{a}(\nu) &= [e^{-j\pi\mathbb{P}_{(y,0)}\nu}, \cdots, e^{-j\pi\mathbb{P}_{(y,M_y-1)}\nu}]^{\mathrm{T}} \in \mathbb{C}^{M_y},\end{aligned} \quad (3)$$

where $\mu = \sin(\phi)\cos(\theta)$, $\nu = \sin(\phi)\sin(\theta)$, and $\mathbb{P}_{(x,i)}$ and $\mathbb{P}_{(y,i)}$ denote the location of the ith sensor from $\mathbb{P}_x$ and $\mathbb{P}_y$, respectively. Therefore, the signals received at the array $\mathbb{S}$ at time t can be expressed as

$$\begin{aligned}\boldsymbol{X}(t) =& \sum_{l=1}^{L} \alpha_l s_c(t) \boldsymbol{a}(\mu_c^l) \circ \boldsymbol{a}(\nu_c^l) + \sum_{d=1}^{D} s_u^d(t) \boldsymbol{a}(\mu_u^d) \circ \boldsymbol{a}(\nu_u^d)\\ &+ \boldsymbol{W}(t) \in \mathbb{C}^{M_x\times M_y},\end{aligned} \quad (4)$$

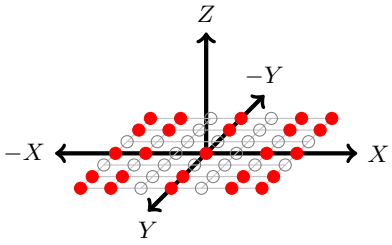

Fig. 1: Array configuration

where $\boldsymbol{W}(t)$ is the noise matrix.

Due to the non-uniformity of the sparse array, it is required to perform array interpolation to apply traditional DOA estimation methods. The interpolation is performed by augmenting virtual sensors in the integer multiple of the half-wavelength region spanned by the array $\mathbb{S}$. The resultant interpolated array can be expressed as

$$\mathbb{U} = \{(x_{\mathbb{U}}, y_{\mathbb{U}}) \mid x_{\mathbb{U}} \in \{-U_x, \cdots, U_x\}d, y_{\mathbb{U}} \in \{-U_y, \cdots, U_y\}d\}. \quad (5)$$

The received signal from the 2-D sparse array $\mathbb{S}$ can be augmented to obtain the received signal from the interpolated uniform rectangular array (URA) $\mathbb{U}$. Let

$$\langle \boldsymbol{Y}(t)\rangle_{(x_{\mathbb{U}},y_{\mathbb{U}})} = \begin{cases}\langle \boldsymbol{X}(t)\rangle_{(x_{\mathbb{U}},y_{\mathbb{U}})}, & (x_{\mathbb{U}}, y_{\mathbb{U}})d \in \mathbb{P},\\ 0, & (x_{\mathbb{U}}, y_{\mathbb{U}})d \in \mathbb{U}\backslash\mathbb{P},\end{cases} \quad (6)$$

where $\langle\cdot\rangle_{(x_{\mathbb{U}},y_{\mathbb{U}})}$ denotes the element corresponding to the sensor location at $(x_{\mathbb{U}}, y_{\mathbb{U}})d$. A binary matrix $\boldsymbol{B}$ is defined to distinguish the virtual and physical sensors in the interpolated URA as

$$\langle \boldsymbol{B}\rangle_{(x_{\mathbb{U}},y_{\mathbb{U}})} = \begin{cases}1, & (x_{\mathbb{U}}, y_{\mathbb{U}})d \in \mathbb{P},\\ 0, & (x_{\mathbb{U}}, y_{\mathbb{U}})d \in \mathbb{U}\backslash\mathbb{P},\end{cases} \quad (7)$$

and its tensor version, denoted as $\boldsymbol{\mathcal{B}}$, is derived by replicating the matrix $\boldsymbol{B}$ in additional dimensions.

Therefore, the initialized signal matrix $\boldsymbol{Y}(t)$ can be related to the signal matrix of the full URA $\mathbb{U}$ as

$$\boldsymbol{Y}(t) = \boldsymbol{B} \odot \boldsymbol{X}_{\mathbb{U}}(t), \quad (8)$$

where $\boldsymbol{X}_{\mathbb{U}}(t)$ is the signal matrix of the full URA. Denoting $\boldsymbol{a}_{\mathbb{U}}(\mu)$ and $\boldsymbol{a}_{\mathbb{U}}(\nu)$ as the steering vectors respectively in the X and Y directions corresponding to the full URA $\mathbb{U}$, the covariance tensor of the initialized signal matrix $\boldsymbol{Y}(t)$ is expressed as

$$\begin{aligned}\boldsymbol{\mathcal{R}} =& \boldsymbol{\mathcal{B}} \odot \Bigg\{\sigma_s^2 \sum_{l=1}^{L}\sum_{l'=1}^{L} \alpha_l^* \alpha_{l'} \boldsymbol{a}_{\mathbb{U}}(\mu_c^{l'}) \circ \boldsymbol{a}_{\mathbb{U}}(\nu_c^{l'}) \circ \boldsymbol{a}_{\mathbb{U}}^*(\mu_c^l) \circ \boldsymbol{a}_{\mathbb{U}}^*(\nu_c^l)\\ &+ \sum_{d=1}^{D} \sigma_{sd}^2 \boldsymbol{a}_{\mathbb{U}}(\mu_u^d) \circ \boldsymbol{a}_{\mathbb{U}}(\nu_u^d) \circ \boldsymbol{a}_{\mathbb{U}}^*(\mu_u^d) \circ \boldsymbol{a}_{\mathbb{U}}^*(\nu_u^d) + \sigma_n^2 \boldsymbol{\mathcal{I}}\Bigg\}\\ &\in \mathbb{C}^{(2U_x+1)\times(2U_y+1)\times(2U_x+1)\times(2U_y+1)},\end{aligned} \quad (9)$$

where $\sigma_s^2 = \mathrm{E}(|s_c(t)|^2)$ is the power of the reference signal of the coherent signal components and $\sigma_{sd}^2 = \mathrm{E}(|s_u^d(t)|^2)$ is the power of the dth uncorrelated signal. The covariance tensor encompasses contributions from both the coherent components and the uncorrelated signals. The presence of cross-terms among the coherent components hinders the covariance tensor from conforming to a full-rank CP problem and, therefore, renders the tensor to be rank-deficient.

3. DOA ESTIMATION

The process of estimating the DOAs for both the coherent group and the uncorrelated signals is carried out through a two-step approach. We first estimate the DOAs of the uncorrelated signals by employing a subspace-based technique, namely, the MUSIC algorithm. We then eliminate the contributions of the uncorrelated signals by considering the conjugate symmetric property of the covariance tensor associated with the uncorrelated signals in a symmetric array. These two steps are briefly discussed in the following subsections.

3.1. DOA Estimation of Uncorrelated Signals

In this section, we consider the covariance tensor that only corresponds to the physically present sensors, i.e., the covariance tensor in (9) is squeeze by removing the 0 elements corresponding to the holes. The covariance tensor corresponding to the physical array is reshaped into a covariance matrix $\boldsymbol{R} \in \mathbb{C}^{M_x M_y \times M_x M_y}$. As signals arriving from the coherent group yield a rank-1 component, the covariance matrix can be partitioned into signal and noise subspaces as

$$\boldsymbol{R} = \boldsymbol{U}_s \boldsymbol{\Lambda}_s \boldsymbol{U}_s^{\mathrm{H}} + \boldsymbol{U}_n \boldsymbol{\Lambda}_n \boldsymbol{U}_n^{\mathrm{H}}, \tag{10}$$

where $\boldsymbol{U}_s$ represents the signal subspace comprising $D+1$ dominant eigenvectors of $\boldsymbol{R}$, while $\boldsymbol{U}_n$ is the noise subspace consisting of the remaining $M_x M_y - D - 1$ eigenvectors. $\boldsymbol{\Lambda}_s$ and $\boldsymbol{\Lambda}_n$ are diagonal matrices consisting of signal and noise eigenvalues, respectively. As multiple coherent signal components form combined steering vectors $\boldsymbol{a}(\mu_c) = \sum_{l=1}^{L} \boldsymbol{a}(\mu_c^l)$ and $\boldsymbol{a}(\nu_c) = \sum_{l=1}^{L} \boldsymbol{a}(\nu_c^l)$, these vectors fail to establish a valid manifold and thus do not exhibit a significant presence in the MUSIC spectra. As a result, the DOAs of the uncorrelated signals can be obtained from the peak locations of the MUSIC spectrum.

3.2. Eliminating the Contribution of Uncorrelated Signals

The contribution of uncorrelated signals to the covariance tensor can be eliminated by recognizing the conjugate symmetric property of the covariance tensor. The covariance tensor $\boldsymbol{\mathcal{R}}$ in (9) can be decomposed into two parts, namely, uncorrelated part $\boldsymbol{\mathcal{R}}_u$ and coherent part $\boldsymbol{\mathcal{R}}_c$. The (u_x, u_y, u_x', u_y')th element of the uncorrelated part of the covariance tensor can be expressed as

$$\begin{aligned}&\boldsymbol{\mathcal{R}}_u(u_x, u_y, u_x', u_y') \\ &= b \left\{ \sum_{d=1}^{D} \sigma_{sd}^2 e^{-j\pi(u_x - u_x')\mu_u^d} e^{-j\pi(u_y - u_y')\nu_u^d} + \sigma_n^2 \zeta_{(u_x,u_y,u_x',u_y')} \right\},\end{aligned} \tag{11}$$

where $u_x, u_x' \in \{-U_x, \cdots, U_x\}$, $u_y, u_y' \in \{-U_y, \cdots, U_y\}$, $b = \boldsymbol{\mathcal{B}}(u_x, u_y, u_x', u_y')$, and $\zeta_{(u_x,u_y,u_x',u_y')}$ equals 1 if $u_x = u_x'$ and $u_y = u_y'$ and equals 0 otherwise. It is noticed that the uncorrelated components of the covariance tensor exhibit conjugate symmetric property, i.e., $\boldsymbol{\mathcal{R}}_u(u_x, u_y, u_x', u_y') = \boldsymbol{\mathcal{R}}_u^*(-u_x, -u_y, -u_x', -u_y')$.

On the other hand, the (u_x, u_y, u_x', u_y')th element of the coherent part can be expressed as

$$\begin{aligned}\boldsymbol{\mathcal{R}}_c(u_x, u_y, u_x', u_y') &= b \left\{ \sigma_s^2 \sum_{l'=1}^{L} \alpha_{l'} e^{-j\pi u_x \mu_{l'}} e^{-j\pi u_y \nu_{l'}} \right. \\ &\quad \left. \cdot \sum_{l=1}^{L} \alpha_l^* e^{j\pi u_x' \mu_l} e^{j\pi u_y' \nu_l} + \sigma_n^2 \zeta_{(u_x,u_y,u_x',u_y')} \right\} \\ &= b \left\{ k_{(u_x,u_y)} \sum_{l=1}^{L} \alpha_l^* e^{j\pi u_x' \mu_l} e^{j\pi u_y' \nu_l} + \sigma_n^2 \zeta_{(u_x,u_y,u_x',u_y')} \right\},\end{aligned} \tag{12}$$

where $k_{(u_x,u_y)} = \sigma_s^2 \sum_{l'=1}^{L} \alpha_{l'} e^{-j\pi u_x \mu_{l'}} e^{-j\pi u_y \nu_{l'}}$ depends only on the first two indices (u_x, u_y) of the covariance tensor. Clearly, the coherent part $\boldsymbol{\mathcal{R}}_c$ does not share the conjugate symmetric property. Therefore, subtracting the conjugate symmetric components from the covariance tensor $\boldsymbol{\mathcal{R}}$ would eliminate the contribution of uncorrelated signals, and the remaining difference covariance tensor, expressed as

$$\begin{aligned}&\boldsymbol{\mathcal{Z}}(u_x, u_y, u_x', u_y') \\ &= \boldsymbol{\mathcal{R}}(u_x, u_y, u_x', u_y') - \boldsymbol{\mathcal{R}}^*(-u_x, -u_y, -u_x', -u_y') \\ &= b \left\{ \sigma_s^2 \sum_{l=1}^{L} q_{(u_x,u_y),l}\, e^{j\pi u_x' \mu_l} e^{j\pi u_y' \nu_l} + \epsilon \right\},\end{aligned} \tag{13}$$

will correspond only to the coherent signal components, where $q_{(u_x,u_y),l} = \sum_{l'=1}^{L} (\alpha_{l'} \alpha_l^* - \alpha_{l'}^* \alpha_l) e^{-j\pi u_x \mu_{l'}} e^{-j\pi u_y \nu_{l'}}$, and ϵ represents the error due to the limited number of snapshots.

3.3. Decorrelation of Coherent Covariance Tensor via Structural Tensor Reconstruction

We employ a tensor reconstruction strategy, similar to the one described in [27], to decorrelate the tensor $\boldsymbol{\mathcal{Z}}$ and obtain a Hermitian Toeplitz tensor $\boldsymbol{\mathcal{D}} \in \mathbb{C}^{(U_x+1)\times(U_y+1)\times(U_x+1)\times(U_y+1)}$ so that a full rank-L CP problem can be formulated. By fixing the first two indices of $\boldsymbol{\mathcal{Z}}$ as (u_x, u_y), i.e., $\boldsymbol{\mathcal{Z}}(u_x, u_y, :, :)$, tensor $\boldsymbol{\mathcal{D}}$ is constructed by rearranging its elements. More specifically, the $(-\tilde{u}_x + \tilde{u}_x')$th row of $\boldsymbol{\mathcal{Z}}(u_x, u_y, :, :)$ can be exploited as the $(\tilde{u}_x, :, \tilde{u}_x', :)$th slice of $\boldsymbol{\mathcal{D}}_{(u_x,u_y)}$. Similarly, the $(-\tilde{u}_y + \tilde{u}_y')$th column of $\boldsymbol{\mathcal{Z}}(u_x, u_y, :, :)$ is utilized to construct the $(:, \tilde{u}_y, :, \tilde{u}_y')$th slice of $\boldsymbol{\mathcal{D}}_{(u_x,u_y)}$. In summary, the mapping between $\boldsymbol{\mathcal{Z}}(u_x, u_y, :, :)$ and $\boldsymbol{\mathcal{D}}_{(u_x,u_y)}$ can be expressed as

$$\boldsymbol{\mathcal{D}}_{(u_x,u_y)}(\tilde{u}_x, \tilde{u}_y, \tilde{u}_x', \tilde{u}_y') = \boldsymbol{\mathcal{Z}}(u_x, u_y, -\tilde{u}_x + \tilde{u}_x', -\tilde{u}_y + \tilde{u}_y'), \tag{14}$$

where $\tilde{u}_x, \tilde{u}_x' \in \{0, \cdots, U_x\}$ and $\tilde{u}_y, \tilde{u}_y' \in \{0, \cdots, U_y\}$.

Substituting (13) into (14), the reconstructed tensor $\boldsymbol{\mathcal{D}}_{(u_x,u_y)}$ can be expressed as

$$\begin{aligned}&\boldsymbol{\mathcal{D}}_{(u_x,u_y)}(\tilde{u}_x, \tilde{u}_y, \tilde{u}_x', \tilde{u}_y') \\ &= b \left\{ \sum_{l=1}^{L} q_{(u_x,u_y),l}\, e^{j\pi(-\tilde{u}_x + \tilde{u}_x')\mu_l} e^{j\pi(-\tilde{u}_y + \tilde{u}'y)\nu_l} + \epsilon \right\}.\end{aligned} \tag{15}$$

Tensor $\boldsymbol{\mathcal{D}}_{(u_x,u_y)}$ exhibits a tensorial Hermitian and Toeplitz structure. Accordingly, $\boldsymbol{\mathcal{D}}_{(u_x,u_y)}$ can be represented as

$$\boldsymbol{\mathcal{D}}_{(u_x,u_y)} = b \left\{ \sum_{l=1}^{L} q_{(u_x,u_y),l}\, \boldsymbol{g}(\mu_l) \circ \boldsymbol{g}(\nu_l) \circ \boldsymbol{g}^*(\mu_l) \circ \boldsymbol{g}^*(\nu_l) + \epsilon \right\}, \tag{16}$$

where $\boldsymbol{g}(\mu_l) = [1, \cdots, e^{-j\pi U_x \mu_l}]^{\mathrm{T}} \in \mathbb{C}^{(U_x+1)}$ and $\boldsymbol{g}(\nu_l) = [1, \cdots, e^{-j\pi U_y \nu_l}]^{\mathrm{T}} \in \mathbb{C}^{(U_y+1)}$ act as the azimuth and elevation steering vectors for the lth coherent signal. Eq. (16) is a rank-L CP problem, and the steering vectors can be estimated by employing CPD on $\boldsymbol{\mathcal{D}}_{(u_x,u_y)}$. Based on the estimated steering vectors, the DOA information can be subsequently estimated. However, due to the missing sensors, tensor $\boldsymbol{\mathcal{D}}_{(u_x,u_y)}$ contains holes. These missing elements in $\boldsymbol{\mathcal{D}}_{(u_x,u_y)}$ are interpolated as in [28] before applying the CPD.

4. SIGNAL IDENTIFIABILITY

To identify the uncorrelated signal, the number of eigenvectors in signal subspace $\boldsymbol{U}_s$ associated with the covariance matrix in (10),

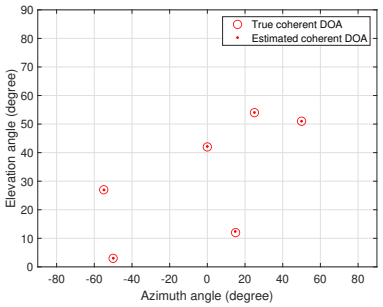

(a) 6 coherent signals

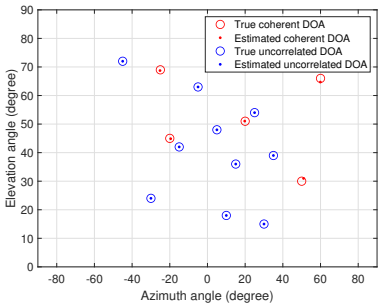

(b) 5 coherent and 10 uncorrelated signals

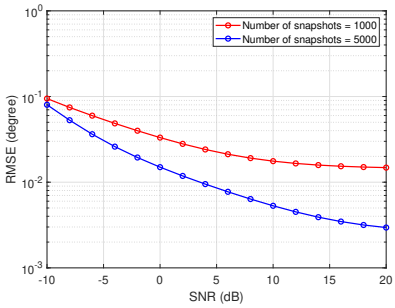

(c) RMSE versus input SNR

Fig. 2: DOA estimation performance.

i.e., $D+1$, should satisfy the following criterion,

$$D+1 \leq M_x M_y - 1. \tag{17}$$

Consequently, the maximum number of uncorrelated signals that can be identified in the presence of a single coherent signal group is $M_x M_y - 2$.

The maximum number of identifiable coherent signals using the proposed method relies on the uniqueness of the CPD of $\boldsymbol{\mathcal{D}}_{(u_x,u_y)}$. Denote the estimated CP factor matrices as $\hat{\boldsymbol{G}}(\mu) = [\hat{\boldsymbol{g}}(\mu_1), \hat{\boldsymbol{g}}(\mu_2), \ldots, \hat{\boldsymbol{g}}(\mu_L)]$ and $\hat{\boldsymbol{G}}(\nu) = [\hat{\boldsymbol{g}}(\nu_1), \hat{\boldsymbol{g}}(\nu_2), \ldots, \hat{\boldsymbol{g}}(\nu_L)]$, where $\hat{\boldsymbol{g}}(\mu_l)$ and $\hat{\boldsymbol{g}}(\nu_l)$ are the estimated steering vectors. These matrices, along with their conjugates $\hat{\boldsymbol{G}}^*(\mu)$ and $\hat{\boldsymbol{G}}^*(\nu)$, have a dimension of $\mathbb{C}^{(U_x+1)\times L}$ and $\mathbb{C}^{(U_y+1)\times L}$, respectively.

The unique estimation of these factor matrices is guaranteed through CPD under the condition [29]:

$$\kappa(\hat{\boldsymbol{G}}(\mu)) + \kappa(\hat{\boldsymbol{G}}(\nu)) + \kappa(\hat{\boldsymbol{G}}^*(\mu)) + \kappa(\hat{\boldsymbol{G}}^*(\nu)) \geq 2L+3, \tag{18}$$

where $\kappa(\hat{\boldsymbol{G}}(\mu)) = \kappa(\hat{\boldsymbol{G}}^*(\mu)) = \min(U_x+1, L)$ and $\kappa(\hat{\boldsymbol{G}}(\nu)) = \kappa(\hat{\boldsymbol{G}}^*(\nu) = \min(U_y+1, L)$. To obtain the upper bound of the number of signals to be detected, we consider the scenario of $U_x + 1 \leq L$ and $U_y + 1 \leq L$. In this case, Eq. (18) becomes $2U_x + 2U_y + 4 \geq 2L + 3$, i.e., $L \leq U_x + U_y + 1/2$. Since L takes an integer value, the maximum number of coherent signals that can be identified becomes

$$L \leq U_x + U_y. \tag{19}$$

Combining (17) and (19), the maximum number of detectable mixed uncorrelated and coherent signals using the proposed approach is given by

$$\text{DOF} \leq M_x M_y + U_x + U_y - 2. \tag{20}$$

5. SIMULATION RESULTS

We consider a 2-D sparse array with the numbers of sensors in the X- and Y-axes being $M_x = M_y = 5$. The total number of sensors is $M_x M_y = 25$. The sensors are positioned in both axes at $\mathbb{P}_x = \mathbb{P}_y = \{-3, -2, 0, 2, 3\}d$. The numbers of elements in the X and Y axes for the interpolated URA are $2U_x + 1 = 2U_y + 1 = 7$ with $U_x = U_y = 3$. Therefore, the proposed approach can identify up to $U_x + U_y = 6$ coherent signal components in a single coherent group and $M_x M_y - 2 = 23$ uncorrelated signals.

To estimate the DOAs involving a mixture of coherent and uncorrelated signals, after identifying the uncorrelated signals using the MUSIC algorithm, the difference covariance tensor $\boldsymbol{\mathcal{Z}}$ is obtained. Without loss of generality, the $(1,1)$th slice of $\boldsymbol{\mathcal{Z}}$, i.e., $\boldsymbol{\mathcal{Z}}_{(1,1,:,:)}$, is utilized to obtain the decorrelated tensor $\boldsymbol{\mathcal{D}}_{(1,1)} \in \mathbb{C}^{4\times4\times4\times4}$. Subsequently, CPD is performed on $\boldsymbol{\mathcal{D}}_{(1,1)}$ to estimate the steering vectors, which are then used to obtain the signal DOAs. We use MATLAB Tensorlab 3 Toolbox [30] to implement CPD on the decorrelated tensor derived through the structural reconstruction approach. The optimization of factor matrices is carried out using the alternating least squares algorithm [31]. Unless otherwise specified, the input signal-to-noise ratio (SNR) is 10 dB, and 1,000 snapshots are used.

Fig. 2(a) considers a scenario involving 6 coherent signal components and Fig. 2(b) depicts a scenario with 5 coherent components and 10 uncorrelated signals. In both cases, successful identification of all signals is evident through the utilization of the proposed method.

The estimation performance is further evaluated in terms of the root mean-squared error (RMSE), expressed as

$$\text{RMSE} = \sqrt{\frac{1}{EQ}\sum_{e=1}^{E}\sum_{q=1}^{Q}\left[(\theta_q - \hat{\theta}_{q,e})^2 + (\phi_q - \hat{\phi}_{q,e})^2\right]}, \tag{21}$$

where E is the number of Monte Carlo trials. We consider 10 mixed signals with 3 coherent components and 7 uncorrelated signals for the RMSE evaluation.

Fig. 2(c) depicts the RMSE values as the input SNR varies between -10 dB and 20 dB. It is evident in the figure that the proposed method achieves low RMSE values when the input SNR is higher and there is a floor limited by the number of snapshots. Therefore, an increase in the number of snapshots leads to a reduction in the RMSE floor.

6. CONCLUSION

This paper utilized tensor decomposition methods to estimate the 2-D DOAs considering a mixed coherent and uncorrelated signal scenario. After detecting the uncorrelated signals using a subspace-based method, we proposed a structural tensor reconstruction-based decorrelation procedure for the DOA estimation of coherent signal components. Exploiting the structural characteristics of multi-dimensional signals through a CPD tensor modeling approach, the proposed method achieved high estimation performance. The effectiveness of the proposed method was assessed through the identifiability condition analysis and simulation results.

7. REFERENCES

[1] D. H. Johnson, *Array Signal Processing: Concepts and Techniques*. Prentice-Hall, 1993.

[2] H. L. Van Trees, *Optimum Array Processing: Part IV of Detection, Estimation, and Modulation Theory*. Wiley, 2002.

[3] T. E. Tuncer and B. Friedlander, *Classical and Modern Direction-of-Arrival Estimation*. Academic Press, 2009.

[4] M. G. Amin, X. Wang, Y. D. Zhang, F. Ahmad, and E. Aboutanios, "Sparse array and sampling for interference mitigation and DOA estimation in GNSS," *Proc. IEEE*, vol. 104, no. 6, pp. 1302–1317, June 2016.

[5] K. Yu, R. E. Hudson, Y. D. Zhang, K. Yao, C. Taylor, and Z. Wang, "Low-complexity 2D direction-of-arrival estimation for acoustic sensor arrays," *IEEE Signal Process. Lett.*, vol. 23, no. 12, pp. 1791–1795, 2016.

[6] S. Sun, A. P. Petropulu, and H. V. Poor, "MIMO radar for advanced driver-assistance systems and autonomous driving: Advantages and challenges," *IEEE Signal Process. Mag.*, vol. 37, no. 4, pp. 98–117, 2020.

[7] S. Sun and Y. D. Zhang, "4D automotive radar sensing for autonomous vehicles: A sparsity-oriented approach," *IEEE J. Sel. Topics Signal Process.*, vol. 15, no. 4, pp. 879–891, 2021.

[8] ——, "Four-dimensional high-resolution automotive radar imaging exploiting joint sparse-frequency and sparse-array design," in *Proc. IEEE Intl. Conf. Acousti., Speech, Signal Process. (ICASSP)*, Toronto, Canada, June 2021, pp. 8413–8417.

[9] R. Schmidt, "Multiple emitter location and signal parameter estimation," *IEEE Trans. Antennas Propag.*, vol. 34, no. 3, pp. 276–280, 1986.

[10] R. Roy and T. Kailath, "Esprit-estimation of signal parameters via rotational invariance techniques," *IEEE Trans. Acousti., Speech, Signal process.*, vol. 37, no. 7, pp. 984–995, 1989.

[11] T.-J. Shan, M. Wax, and T. Kailath, "On spatial smoothing for direction-of-arrival estimation of coherent signals," *IEEE Trans. Acousti., Speech, Signal Process.*, vol. 33, no. 4, pp. 806–811, 1985.

[12] Y.-M. Chen, "On spatial smoothing for two-dimensional direction-of-arrival estimation of coherent signals," *IEEE Trans. Signal Process.*, vol. 45, no. 7, pp. 1689–1696, 1997.

[13] F.-M. Han and X.-D. Zhang, "An ESPRIT-like algorithm for coherent DOA estimation," *IEEE Antennas Wirel. Propag. Lett.*, vol. 4, pp. 443–446, 2005.

[14] F.-J. Chen, S. Kwong, and C.-W. Kok, "ESPRIT-like two-dimensional DOA estimation for coherent signals," *IEEE Trans. Aerosp. Electron. Syst.*, vol. 46, no. 3, pp. 1477–1484, 2010.

[15] X. Xu, Z. Ye, Y. Zhang, and C. Chang, "A deflation approach to direction of arrival estimation for symmetric uniform linear array," *IEEE Antennas Wirel. Propag. Lett.*, vol. 5, pp. 486–489, 2006.

[16] S. Qin, Y. D. Zhang, and M. G. Amin, "DOA estimation of mixed coherent and uncorrelated targets exploiting coprime MIMO radar," *Digital Signal Process.*, vol. 61, pp. 26–34, 2017.

[17] Q. Wu, Y. D. Zhang, M. G. Amin, and B. Himed, "Complex multitask bayesian compressive sensing," in *Proc. IEEE Int. Conf. Acousti., Speech, Signal Process. (ICASSP)*, Florence, Italy, May 2014, pp. 3375–3379.

[18] J. D. Carroll and J.-J. Chang, "Analysis of individual differences in multidimensional scaling via an N-way generalization of 'Eckart-Young' decomposition," *Psychometrika*, vol. 35, no. 3, pp. 283–319, 1970.

[19] R. A. Harshman, "Foundations of the PARAFAC procedure: Models and conditions for an 'explanatory' multimodal factor analysis," *UCLA Work. Papers Phonetics*, vol. 16, pp. 1–84, 1970.

[20] L. R. Tucker, "Some mathematical notes on three-mode factor analysis," *Psychometrika*, vol. 31, no. 3, pp. 279–311, 1966.

[21] L. De Lathauwer, B. De Moor, and J. Vandewalle, "A multilinear singular value decomposition," *SIAM J. Matrix Anal. Appl.*, vol. 21, no. 4, pp. 1253–1278, 2000.

[22] N. D. Sidiropoulos, R. Bro, and G. B. Giannakis, "Parallel factor analysis in sensor array processing," *IEEE Trans. Signal Process.*, vol. 48, no. 8, pp. 2377–2388, 2000.

[23] H. Zheng, C. Zhou, Z. Shi, Y. Gu, and Y. D. Zhang, "Coarray tensor direction-of-arrival estimation," *IEEE Trans. Signal Process.*, vol. 71, pp. 1128–1142, 2023.

[24] H. Zheng, Z. Shi, C. Zhou, and A. L. de Almeida, "Coarray tensor completion for DOA estimation," *IEEE Trans. Aerosp. Electron. Syst.*, 2023.

[25] Y. Lin, S. Jin, M. Matthaiou, and X. You, "Tensor-based channel estimation for millimeter wave MIMO-OFDM with dual-wideband effects," *IEEE Trans. Commun.*, vol. 68, no. 7, pp. 4218–4232, 2020.

[26] W. Sun, H. C. So, F. K. W. Chan, and L. Huang, "Tensor approach for eigenvector-based multi-dimensional harmonic retrieval," *IEEE Trans. Signal Process.*, vol. 61, no. 13, pp. 3378–3388, 2013.

[27] H. Zheng, C. Zhou, Z. Shi, and Y. Gu, "Structured tensor reconstruction for coherent DOA estimation," *IEEE Signal Process. Lett.*, vol. 29, pp. 1634–1638, 2022.

[28] C. Zhou, Y. Gu, Z. Shi, and Y. D. Zhang, "Off-grid direction-of-arrival estimation using coprime array interpolation," *IEEE Signal Processing Letters*, vol. 25, no. 11, pp. 1710–1714, 2018.

[29] N. D. Sidiropoulos and R. Bro, "On the uniqueness of multilinear decomposition of N-way arrays," *J. Chemometr.*, vol. 14, no. 3, pp. 229–239, 2000.

[30] N. Vervliet, O. Debals, L. Sorber, M. Van Barel, and L. De Lathauwer. Tensorlab 3.0 (March 2016). [Online]. Available: https://www.tensorlab.net

[31] L. De Lathauwer and D. Nion, "Decompositions of a higher-order tensor in block terms—Part III: Alternating least squares algorithms," *SIAM J. Matrix Anal. Appl.*, vol. 30, no. 3, pp. 1067–1083, 2008.